Interstitially-Stabilized Praseodymium(III) Compounds $Na_2Pr_4Br_9NO$ and $Pr_8Br_{13}N_3O$: Structures on the Border between Salts and Clusters

Michael Lulei, Sharon J. Steinwand, and John D. Corbett*

Department of Chemistry, Iowa State University, Ames, Iowa 50011

Received December 13, 1994[⊗]

The title compounds are obtained in high yields after appropriate reactions in sealed Nb tubing at ~750–950 °C in nonreduced systems but only when both O and N sources are included in the appropriate proportions. The structures of both have been established by single crystal means. ($Na_2Pr_4Br_9NO$: $P2_1/m$, $Z = 2$, $a = 8.543(4)$ Å, $b = 11.707(3)$ Å, $c = 9.697(4)$ Å, $\beta = 106.49(3)$ °, R, $R_w = 3.7$, 4.9%. $Pr_8Br_{13}N_3O$: $C2/c$, $Z = 4$, $a = 21.967(8)$ Å, $b = 8.355(2)$ Å, $c = 16.889(7)$, $\beta = 119.40(3)$ °, R, $R_w = 2.9$, 3.1%.) The former is isotypic (but not isoelectronic) with the known $Na_2Pr_4Cl_9O_2$. Both phases contain infinite zigzag chains of N- and O-centered Pr_4 tetrahedra sharing trans edges, and both appear to be Pr^{III} valence compounds. They can also be geometrically related to reduced compounds like Pr_4I_5Ru with infinite octahedral chains and are thus on the borderline between reduced, metal-rich cluster phases and "simple" salts.

Introduction

The presence of adventitious impurities such as carbon and nitrogen was an important factor in the early syntheses of reduced rare-earth-metal cluster halides. These cluster phases evidently never form without the stabilization provided by interstitial atoms. Of course, interstitials are now added by design in attempts to synthesize new phases as well as to modify known phases electronically. However, the discovery of the new structure types reported here proves that the phenomena generated by the "adventitious" interstitial can still provide new and unexpected materials, here valid in particular for oxygen. While boron, carbon, and nitrogen are possible interstitials in a large number of cluster compounds and structures in reduced rare-earth-metal halide systems, oxygen almost always seems to form only simple oxyhalides, e.g., PrOBr, as the stable products in these systems, reduced or not. The exceptions have been M_4OCl_6 (M^{II} = Yb, Eu, Sm)[1,2] and reduced $M_9I_8C_4O$ (M = Y, Ho, Er, Lu)[3] and $Y_7I_6C_3O$[4] with oxygen in tetrahedral metal sites and carbon in octahedral sites. In addition, there is the recent report of $A_2Pr_4Cl_9O_2$ phases, A = Na, K,[5] that are isotypic but evidently not isoelectronic with the first compound reported here. There are, besides, the well-known representatives α-M_2Cl_3N (M = Gd,[6] Y,[7] La–Nd[8]) and β-$M_2Cl_3N_x$ (M = Gd, Y)[7] with infinite chains and double chains, respectively, of edge-sharing M_4N tetrahedral units as well as Gd_3Cl_6N[9] with isolated double tetrahedra Gd_6N_2. Although these compounds all exhibit short M–M distances, none but the $M_9I_8C_4O$, $Y_7I_6C_3O$, and $A_2Pr_4Cl_9O_2$ examples appears to have any electrons for metal–metal bonding; otherwise they are bound only through interactions of both the interstitial and halogen with normal-valent metals and are therefore only loosely termed "cluster compounds".

The new Pr phases described here exhibit features common to the trivalent Gd and Y structures M_2Cl_3N and divalent Eu, Yb, and Sm compounds in M_4OCl_6 as well as to reduced condensed cluster halides like Pr_4I_5Ru.[10] The present examples are novel in that mixed N and O interstitials are necessary to fulfill Pr(III) valence requirements.

Experimental Section

Materials. The rare-earth metals used, the preparation and vacuum sublimation of their tribromides, the reaction techniques in welded Nb tubing, and the Guinier X-ray powder pattern methods have all been described before.[11,12] PrN (prepared by J.-T. Zhao) and Pr_6O_{11} (Ames Laboratory) were characterized by powder diffraction and found to be single phase. The carbon reactant was spectroscopic grade (Union Carbide) while NaN_3 (Aldrich, 99%) was used as a source of nitrogen for the sodium compound. Reagent NaBr (Baker, 99.9%) was dried by slow heating under dynamic vacuum and then sublimed.

Syntheses. $Na_2Pr_4Br_9NO$. The first few irregularly-shaped black crystals were obtained after heating mixtures of NaBr, $PrBr_3$, Pr, and Ru with the stoichiometries "$Na_3Pr_6Br_6Ru_2$" and "$Na_6Pr_6Br_6Ru_2$" for 25 days at 720 °C. The likely sources for N and O were a residual glovebox atmosphere and a slight hydrolysis of $PrBr_3$, respectively. After the structure and composition were established, we accordingly obtained the new phase in high yield (>70%, plus ~10% NaBr, ~10% $PrBr_3$) from similar reactions of $PrBr_3$, NaN_3 (to provide a nitrogen atmosphere), NaBr, Pr_6O_{11} and Pr with an overall stoichiometry of "$Na_2Pr_{3.67}Br_{10}N_3O$" for 21 days at 750 °C. The product occurred as green, transparent crystals, indicating a Pr^{III} compound and thence a 1:1 ratio for N:O. Reactions with NaN_3 or Pr_6O_{11} alone did not yield the new phase. The original black crystals may have been very slightly richer in oxygen, but the lattice constant differences (diffractometer vs Guinier) were all less than 3σ. This and the refinement achieved both preclude a significant Ru content of the original product.

$Pr_8Br_{13}N_3O$. A few black crystals and the same powder pattern component were obtained from runs loaded as either "$Pr_2Br_2Mn_2$" or "$Pr_2Br_2Fe_2$" and reacted at 950 °C for 20 days. Once the structure was determined as $Pr_8Br_{13}Z_4$ (in which the interstitial Z refined best as N), the actual identity of Z (and the certain absence of Mn or Fe) was established from a series of reactions that included the more likely adventitious components C, N, and O. These utilized C, PrN, and Pr_6O_{11} as Z sources. Reactions run under the same conditions as before

[⊗] Abstract published in *Advance ACS Abstracts,* April 15, 1995.

(1) Schleid, Th.; Meyer, G. *J. Less-Common Met.* **1987**, *127*, 161.
(2) Schleid, Th.; Meyer, G. *Z. Anorg. Allg. Chem.* **1987**, *554*, 118.
(3) Mattfeld, H.; Krämer, K.; Meyer, G. *Z. Anorg. Allg. Chem.* **1993**, *619*, 1384.
(4) Mattausch, Hj.; Borrmann, H.; Simon, A. *Z. Naturforsch.* **1993**, *48B*, 1828.
(5) Mattfeld, H.; Meyer, G. *Z. Anorg. Allg. Chem.* **1994**, *620*, 85.
(6) Schwanitz-Schüller, U.; Simon, A. *Z. Naturforsch.* **1985**, *40B*, 705.
(7) Meyer, H.-J.; Jones, N. L.; Corbett, J. D. *Inorg. Chem.* **1989**, *28*, 2635.
(8) Uhrlandt, S.; Meyer, G. *J. Alloys Compd.* in press.
(9) Simon, A.; Koehler, T. *J. Less-Common Met.* **1986**, *116*, 279.
(10) Payne, M. W.; Dorhout, P. K.; Corbett, J. D. *Inorg. Chem.* **1991**, *30*, 1467.
(11) Payne, M. W.; Corbett, J. D. *Inorg. Chem.* **1990**, *29*, 2246.
(12) Corbett, J. D. *Inorg. Synth.* **1983**, *22*, 15, 31.

0020-1669/95/1334-2671$09.00/0

with either C or O or both did not yield the new phase, while three that included various amounts of PrN gave <10% to ~30% of $Pr_8Br_{13}Z_4$, greatest for "$Pr_8Br_{14}N_{3.3}$", plus ~10% PrOBr and a substantial amount of an unknown product. (The oxygen probably came from both a slight hydrolysis of the $PrBr_3$ and the small amounts of H_2O that slowly but continuously evolve at this temperature from the fused silica jacket around the niobium container.) Addition of Pr_6O_{11} to one of these product mixtures to afford N:O = 3:1 followed by a repeat reaction increased the yield to ~75%. (No reducing agent was included with the oxide, so some oxygen presumably went to form NbO_x.) The dark product crystals ground to an off-white powder. The composition $Pr_8Br_{13}N_3O$ corresponds to a normal-valent praseodymium(III) phase with oxide and nitride interstitials.

X-ray Studies. Some of the first single crystals of $Na_2Pr_4Br_9NO$ and $Pr_8Br_{13}N_3O$ obtained (above) through the intrusion of unknown adventitious impurities were sealed inside thin-walled capillaries under a nitrogen atmosphere and found to be suitable for X-ray diffraction experiments with the aid of oscillation and Laue film checks. Diffraction data for each were collected at room temperature with the aid of a Rigaku AFC6R diffractometer and graphite-monochromated Mo Kα radiation from a 12-kW rotating anode generator. Cell constants and orientation matrices for data collection were determined from a least-square refinement of the setting angles of 25 centered reflections.

Both structures were solved using direct methods (SHELX[13]). Programs, scattering factors, etc. utilized were those in the instrument package TEXSAN.[14] Empirical absorption corrections were applied to both data sets with the aid of an average of three to six Ψ-scans, and redundant data were averaged. For $Na_2Pr_4Br_9NO$, an anisotropic refinement of the Na position could not be accomplished, and the least-squares refinement with the heavy atoms anisotropic converged at R, R_w = 5.1, 6.5%. The ΔF map revealed a neighboring peak to Na of 7.7 e/Å^3. A Fourier map (supplementary material) showed a significantly elongated peak at this position with two slightly distinguishable maxima of nearly the same size ~0.7 Å apart along b. These were subsequently refined separately as Na1 and Na2 with occupancies and B's of 47(1) and 53% and 0.3(1) and 0.3 (constrained) Å^2, respectively, to yield final residuals of R, R_w = 3.7, 4.9%. The difference map at this point showed peaks of only 3.2 e/Å^3 (1.17 Å from Br5) and −2.4 e/Å^3. Of course, the refinement of such close, overlapping components cannot be expected to be especially precise. The structure cannot be successively refined (or the effect at Na removed) by refinement in the acentric $P2$ or Pm or in triclinic space groups, and a twinning model (about $\bar{1}$) is not suitable either. The two Na sites sensibly correspond to alternate six- and three-coordinate environments, respectively (see Discussion); an ordered superstructure along $\bar{b}$ seemed precluded by oscillation photos normal to that axis taken on the diffractometer. All interstitial sites are equivalent, and so any N/O ordering was not resolved.

The data for $Pr_8Br_{13}N_3O$, were originally collected, and the structure solved and refined, in $\bar{P}1$. Additional symmetry was evident in the model at $R \sim 6\%$. The final anisotropic refinement of the structure in the correct $C2/c$ group (with N/O isotropic) resulted in R, R_w values of 2.9, 3.1% after a DIFABS[15] absorption correction (μ = 332 cm^{-1}). The maximum and minimum peaks in the final difference Fourier calculation were 1.65 e/Å^3 (0.96 Å from Br5) and −1.65 e/Å^3.

The powder patterns calculated for each of the refined structural models agreed very well with those observed for the respective products. Some crystal and refinement details are given in Table 1, and the atom positions and equivalent isotropic ellipsoid values are listed in Tables 2 and 3. More complete diffraction information is included in the supplementary material along with anisotropic displacement parameters; these and the structure factor data are also available from J.D.C.

Results and Discussion

Both structures may be described as being built of infinite chains of trans-edge-sharing Pr_4 tetrahedra that are centered by a mixture of N and O, viz., $^1_\infty[Pr_{4/2}(O,N)]$, and are both sheathed and interconnected by Br atoms.

In $Na_2Pr_4Br_9NO$, the chains of metal tetrahedra lie parallel to each other and along b, which axis contains a 2-fold screw axis. The chains are shown in two nearly orthogonal views in Figures 1 and 2. The tetrahedra are defined by three crystallographically distinct metal atoms with shared (trans) edges Pr1−Pr2 and Pr3−Pr3 and are centered by a light atom and surrounded by six kinds of Br atoms with different functionalities. Figure 1 shows how Br3 and Br4 each have three Pr neighbors and simultaneously bridge two edges (Pr1−Pr3 and Pr2−Pr3, respectively) in the same puckered chain. Br1 atoms bridge a Pr1−Pr3 edge and also form a long exo (i−a) bond along $\vec{a}$ (approximately) to Pr3 in an adjacent chain, while Br6 only bridges a Pr2−Pr3 edge in one chain without bonding contacts to other Pr atoms. As seen in Figure 2, Br5 atoms are

Table 1. Crystallographic Data for $Na_2Pr_4Br_9NO$ and $Pr_8Br_{13}N_3O$

	$Na_2Pr_4Br_9NO$	$Pr_8Br_{13}N_3O$
fw	1358.76	2224.05
space group, Z	$P2_1/m$ (No. 11), 2	$C2/c$ (No. 15), 4
lattice constants[a]		
a (Å)	8.543(4)	21.967(8)
b (Å)	11.707(3)	8.355(2)
c (Å)	9.697(4)	16.889(7)
β (deg)	106.49(3)	119.40(3)
V (Å^3)	930.0(6)	2701(3)
d_{calc}(g/cm^3)	4.85	5.46
μ (Mo Kα, cm^{-1})	294.55	331.67
R, R_w[b]	0.037, 0.049	0.029, 0.031

[a] Cell constants from 22 Guinier powder pattern reflections for $Pr_8Br_{13}N_3O$ and 26 reflections for $Na_2Pr_4Br_9NO$, each measured with Si as internal standard; λ = 1.540 562 Å, 22 °C. [b] $R = \sum||F_o| - |F_c||/\sum|F_o|$; $R_w = [\sum w(|F_o| - |F_c|)^2/\sum w(F_o)^2]^{1/2}$, $w = \sigma_F^{-2}$.

Table 2. Positional and Isotropic Equivalent Displacement Parameters for $Na_2Pr_4Br_9NO$

atom	x	y	z	B_{eq}[a] (Å^2)
Pr1	0.9083(1)	0.25	0.1625(1)	0.88(4)
Pr2	0.8959 (1)	0.25	0.7916(1)	0.94(4)
Pr3	0.2080(1)	0.04113(7)	0.0471(1)	1.14(3)
Na1[b]	0.281 (1)	0.983 (1)	0.573 (1)	0.3(1)
Na2	0.245 (1)	0.043 (1)	0.567 (1)	0.3
Br1	0.6084(2)	0.4012 (1)	0.1224(2)	2.49(7)
Br2	−0.0082(3)	−0.0029(2)	0.6966(2)	3.18(9)
Br3	0.2756(3)	0.25	0.2637(3)	1.8(1)
Br4	0.2561(3)	0.25	0.8564(3)	1.9(1)
Br5	0.8677(5)	0.25	0.4692(3)	4.2(1)
Br6	0.5963(2)	0.0936(2)	0.6857(2)	3.13(8)
N/O	0.942(1)	0.125(1)	0.986(1)	0.9(2)

[a] $B_{eq} = (8\pi^2/3)\sum_i\sum_j U_{ij}a_i^*a_j^*\vec{a}_i\vec{a}_j$. [b] Sodium occupancies are 47(1) and 53(1)%, respectively.

Table 3. Positional and Isotropic Equivalent Displacement Parameters for $Pr_8Br_{13}N_3O$

atom	x	y	z	B_{eq}[a] (Å^2)
Pr1	0.36848(3)	0.42542(8)	0.05601(5)	0.72(2)
Pr2	0.07310(3)	0.32246(8)	0.43956(5)	0.85(2)
Pr3	0.43593(3)	0.46492(8)	0.38449(5)	0.82(2)
Pr4	0.22955(3)	0.27525(8)	0.38641(5)	0.78(2)
Br1	0.20065(6)	0.0970(2)	0.13995(9)	1.23(5)
Br2	0.31381(6)	0.4386(2)	0.18406(9)	1.04(4)
Br3	0.34922(6)	0.1512(2)	0.36200(9)	1.08(4)
Br4	0.46523(6)	0.1726(2)	0.0283(1)	1.64(5)
Br5	0.32270(7)	0.0759(2)	0.0620(1)	2.06(5)
Br6	0.07420(7)	0.3005(2)	0.2273(1)	2.30(5)
Br7	0	0.8686(3)	0.25	1.80(7)
N/O1	0.0472(4)	0.067(1)	0.4641(7)	0.7(2)
N/O2	0.1767(5)	0.187(1)	0.4696(7)	0.7(2)

[a] $B_{eq} = (8\pi^2/3)\sum_i\sum_j U_{ij}a_i^*a_j^*\vec{a}_i\vec{a}_j$.

(13) Sheldrick, G. M. SHELXS-86. Universität Göttingen, Germany, 1986.
(14) TEXSAN, version 6.0, Molecular Structure Corp., The Woodlands: TX, 1990.
(15) Walker, N.; Stuart, D. *Acta Crystallogr.* **1983**, *A39*, 158.

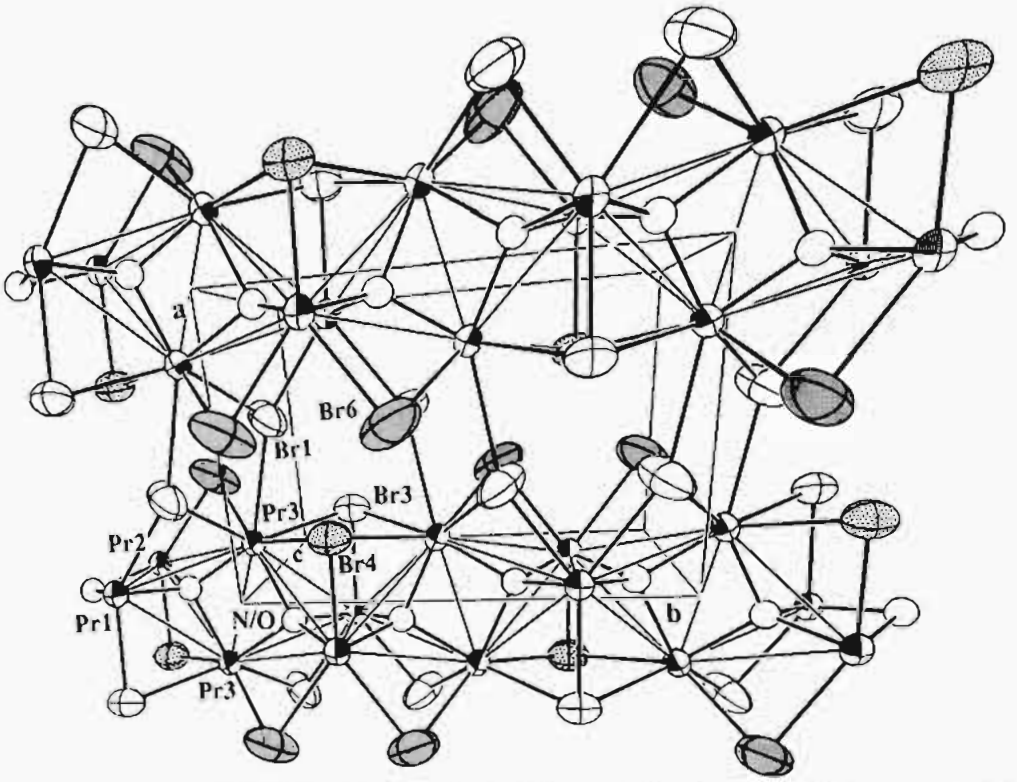

Figure 1. ~[001] view of two 1 $^{1}_{\infty}$[$Pr_{4/2}$(O/N)] chains on the front face of the unit cell in $Na_2Pr_4Br_9NO$. Pr atoms are shaded, Br crossed (Br4 dotted, Br6 gray), and N/O have open ellipsoids (98% probability thermal ellipsoids).

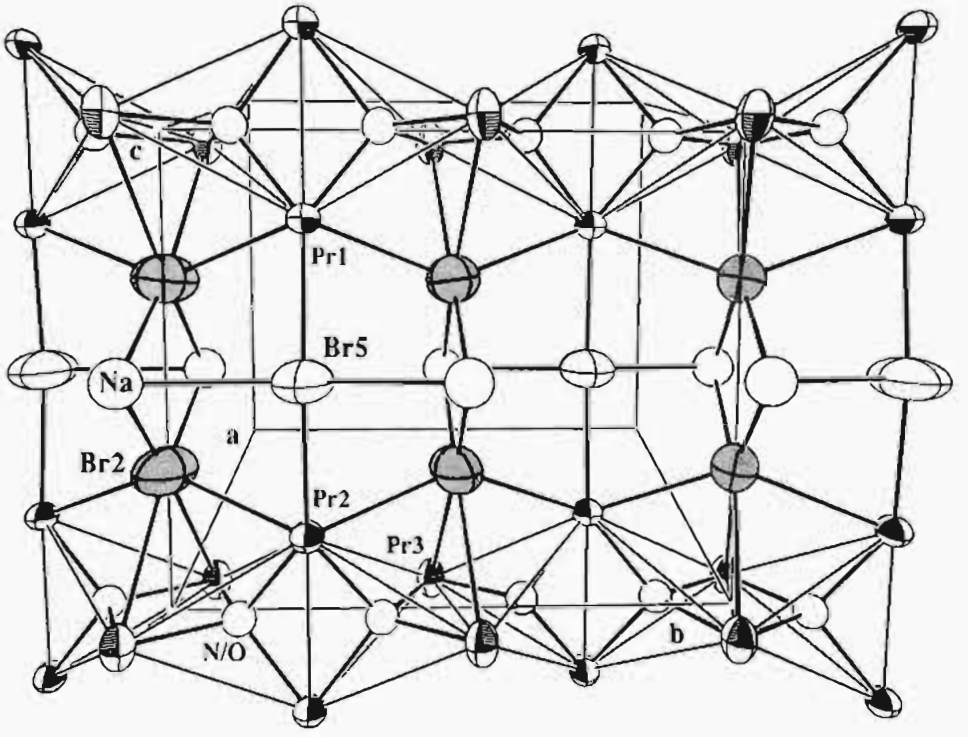

Figure 2. ~[100] view of the chains in $Na_2Pr_4Br_9NO$. Pr, Br, and N/O atoms are keyed the same as in Figure 1 (Br2 is gray), and Na is open.

bonded only along $\bar{c}$ to Pr1 and Pr2 vertices in parallel chains and with fairly short separations (∠Pr1−Br5−Pr2 = 169.5 (2)°), while two Na neighbors complete a slightly distorted square. The odd environment of Br5 is doubtlessly responsible for its thermal ellipsoid elongation along $\bar{a}$, and the two-bonded Br6 behaves similarly. Finally, Br2 atoms fit in the saddles between pairs of tetrahedra (on both sides of the chain) (Figure 2) and thereby cap two faces defined by Pr1 and Pr2 and the shared Pr3−Pr3 edge, these separations all being relatively long. The coordination environments of Pr1 and Pr2 are bicapped trigonal prisms. Each Pr is bonded to two N/O atoms at about 2.33 Å and six Br atoms at 2.96−3.27 Å. Pr3 exhibits a tricapped trigonal prism built by two N/O atoms (2.30, 2.39 Å) and seven Br atoms (3.05−3.42 Å) (Table 4).

The bromine neighbors about each mean Na position define a rather open coordination polyhedron, Figure 3 (top). The sodium cations function as spacers along the *c* axis and bind the tetrahedral chains together in this direction, particularly via

Table 4. Important Distances (Å) in $Na_2Pr_4Br_9NO$

Pr1–Pr2	3.569(2)	**Na1**–Na1	4.37(2)	**Br2**–Pr1	3.210(2)	**N/O**–N/O	2.93(2)
Pr1–Pr3	3.926(2)		4.62(2)	Br2–Pr2	3.273(2)		3.07(2)
	3.948(1)	Na1–Na2	0.76(1)	Br2–Pr3	3.415(3)	N/O–Pr1	2.33(1)
Pr2–Pr3	3.934(2)	**Na2**–Na2	4.14(2)		3.421(3)	N/O–Pr2	2.33(1)
	3.955(1)		4.85(2)	Br2–Na1	2.98(1)	N/O–Pr3	2.30(1)
Pr3–Pr3	3.543(2)				3.04(1)	N/O–Pr3	2.39(1)
	4.890(2)	**Na1**-Br1[c]	2.99(1)	Br2–Na2	2.81(1)		
		Na1-Br2	2.98(1)		2.84(1)		
Pr1–Br1[a,b]	3.047(2)		3.04(1)				
Pr1–Br2[a]	3.210(2)	Na1-Br5	2.99(1)	**Br3**–Pr1	3.011(3)	Shortest Nonbonded	
Pr1–Br3	3.011(3)	Na1–Br6	2.91(1)	Br3–Pr3a	3.168(2)	Distances	
Pr1–Br5	3.091(3)		3.11(1)				
Pr1–N/O[a]	2.33(1)			**Br4**–Pr2	2.961(3)	Br1–Br1	3.452(4)
		Na2–Br1	3.35(1)	Br4–Pr3[a]	3.162(2)	Pr1–Na1	4.36(1)
Pr2–Br2[a]	3.273(2)	Na2–Br2	2.81(1)			Br2–N/O	3.29(1)
Pr2–Br4	2.961(3)		2.84(1)	**Br5**-Pr1	3.091(3)		
Pr2–Br5	3.066(4)	Na2–Br5	3.55(1)	Br5–Pr2	3.066(4)		
Pr2–Br6[a]	3.077(2)	Na2–Br6	2.96(1)	Br5–Na1[a]	2.99(1)		
Pr2–N/O[a]	2.33(1)		3.50(1)	Br5–Na2[a]	3.55(1)		
Pr3–Br1	3.051(2)	**Br1**–Pr1	3.047(2)	**Br6**–Pr2	3.077(2)		
	3.357(3)	Br1–Pr3	3.051(2)	Br6–Pr3	3.089(2)		
Pr3–Br2	3.415(3)		3.357(3)	Br6–Na1	2.91(1)		
	3.421(3)	Br1–Na1	2.99(1)	Br6–Na1	3.11(1)		
Pr3–Br3	3.168(2)	Br1–Na2	3.35(1)	Br6–Na2	2.96(1)		
Pr3–Br4	3.162(2)			Br6–Na2	3.50(1)		
Pr3–Br6	3.089(2)						
Pr3–N/O	2.30(1)						
	2.39(1)						

[a] Distance occurs twice. [b] Additional Pr–Br separations >3.5 Å are omitted. [c] Additional Na–Br separations >3.6 Å are omitted.

Table 5. Important Distances (Å) in $Pr_8Br_{13}N_3O$

Pr1–Pr2	3.544(1)	**Pr3**–Br1	3.029(2)	**Br3**–Pr2	2.929(2)	**N/O2**–N/O2	3.05(2)
Pr1–Pr3	3.955(2)	Pr3–Br2	3.129(2)	Br3–Pr3	3.152(2)	N/O2–Pr1	2.35(1)
	3.917(2)	Pr3–Br3	3.152(2)	Br3–Pr4	3.036(2)	N/O2–Pr2	2.36(1)
Pr1–Pr4	4.023(1)	Pr3–Br4	3.116(2)			N/O2–Pr4	2.34(1)
	3.898(2)	Pr3–Br6	3.326(2)	**Br4**–Pr1	3.190(2)	N/O2–Pr4	2.31(1)
Pr2–Pr3	3.901(2)	Pr3–Br7	3.306(1)	Br4–Pr2	3.164(2)		
	4.015(1)	Pr3–N/O1	2.30(1)		3.369(2)		
Pr2–Pr4	3.948(2)	Pr3–N/O1	2.41(1)	Br4–Pr3	3.116(2)		
	3.975(2)					Shortest Distances	
Pr3–Pr3	3.565(2)	**Pr4**–Br1	3.232(2)	**Br5**–Pr1	3.107(2)		
Pr4–Pr4	3.510(2)	Pr4–Br2	3.020(2)	Br5–Pr2	3.127(2)	Br1–Br2	3.408(2)
		Pr4–Br3	3.036(2)	Br5–Pr4	3.061(2)	Br5–N/O2	3.29(1)
Pr1–Br1[a]	2.891(2)	Pr4–Br5	3.061(2)				
Pr1–Br2	2.946(2)	Pr4–Br6	3.148(2)	**Br6**–Pr2	3.081(2)		
Pr1–Br4	3.190(2)	Pr4–N/O2	2.31(1)	Br6–Pr3	3.326(2)		
Pr1–Br5	3.107(2)		2.34(1)	Br6–Pr4	3.148(2)		
Pr1–Br7	3.164(2)						
Pr1–N/O1	2.36(1)	**Br1**–Pr1	2.891(2)	**Br7**–Pr1[b]	3.164(2)		
Pr1–N/O2	2.35(1)	Br1–Pr3	3.029(2)	Br7–Pr3[b]	3.306(1)		
		Br1–Pr4	3.232(2)				
Pr2–Br3	2.929(2)			**N/O1**–N/O1	3.08(2)		
Pr2–Br4	3.164(2)	**Br2**–Pr1	2.946(2)	N/O1–N/O2	2.97(1)		
	3.369(2)	Br2–Pr3	3.129(2)	N/O1–Pr1	2.36(1)		
Pr2–Br5	3.127(2)	Br2–Pr4	3.020(2)	N/O1–Pr2	2.30(1)		
Pr2–Br6	3.081(2)			N/O1–Pr3	2.30(1)		
Pr2–N/O1	2.30(1)			N/O1–Pr3	2.41(1)		
Pr2–N/O2	2.36(1)						

[a] Additional Pr–Br separations > 3.5 Å are omitted. [b] Distance is observed two times.

the Br2 atoms, Figure 2. The relatively unsuitable environment afforded sodium by the bromine sublattice around the network of bridged chains is reflected in its odd disposition, as shown at the bottom in Figure 3. The refinement indicates ~47% of the Na(1) occupies a plausible but still rather open six-coordinate site with an average Na–Br distance of 3.00 Å. (The sum of crystal radii is 2.98 Å.[16] The longest d(Na–Br) is 3.12 Å to Br6 on the open (Br5) side.) The apparent alternative ~53% of the time is the planar three-coordinate (C_{2v}) Na2 site between Br6 and 2Br2 (d(Na2–Br) = 2.87 Å) which is further into the cavity and 0.76 Å from Na1. (The next closest Br1 is 3.36 Å removed.) The situation is reminiscent of, but not identical to, many situations that have been encountered with cations in poorly proportioned, low symmetry sites in zirconium cluster halide structures.[17,18] This structure shows some interesting differences with respect to that recently reported for the isotypic $A_2Pr_4Cl_9O_2$, A = Na, K.[5,19] The cations in the latter exhibited large ellipsoids (B_{iso} = 5.8, 8.2 Å^2, respectively) which for sodium was elongated by ~5:1 along b,[20] but the distribution was not resolved into split positions as for the bromide, perhaps

(16) Shannon, R. D. *Acta Crystallogr.* **1976**, *A32*, 751.

(17) Ziebarth, R. P.; Corbett, J. D. *Acc. Chem. Res.* **1989**, *22*, 256.

(18) Corbett, J. D. in *Modern Perspectives in Inorganic Crystal Chemistry*; Parthé, E., Ed.; Kluwer Academic Publishers: Dordrecht, The Netherlands, 1992; p. 27.

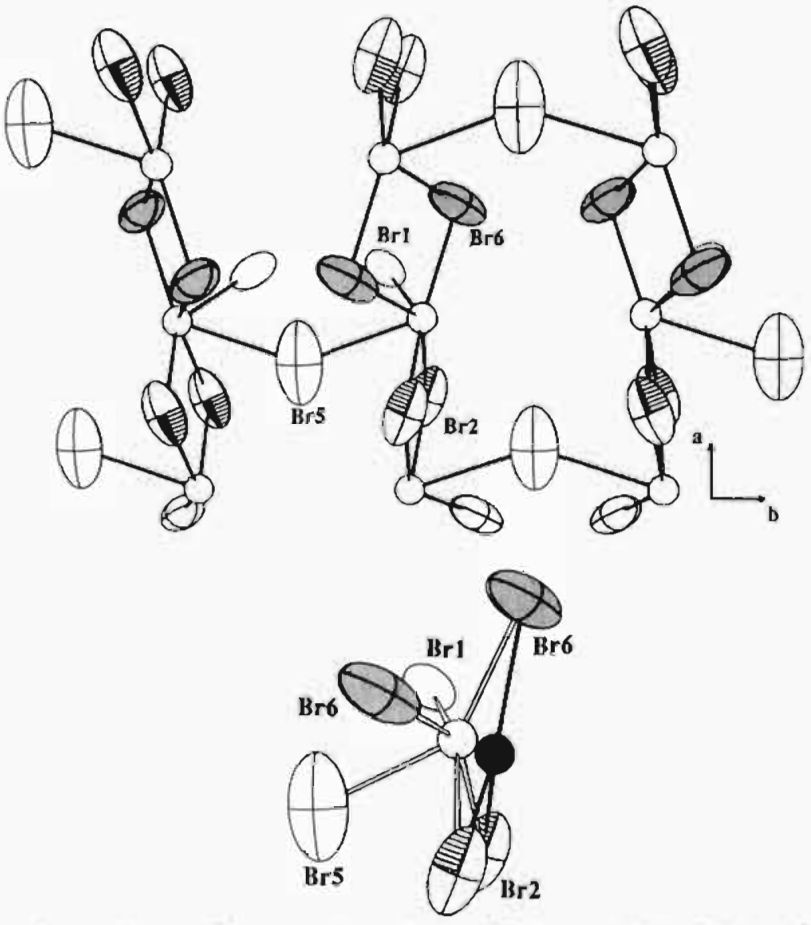

Figure 3. Top: The sodium environment in terms of the mean cation position with Br2 atoms shaded and Br6 gray. $\bar{b}$ is horizontal and in the page. Bottom: The refined Na1 (open sphere, 6-coordinate) and Na2 (solid, 3-coordinate) sites within central bromide polyhedron in the top view.

because of the smaller chloride neighbors. It is conceivable that unrecognized nitrogen interstitials may have been responsible for the no more than 50% yields achieved of the chloride oxide.

In $Pr_8Br_{13}N_3O$, similar zigzag chains of trans-edge-sharing Pr_4 tetrahedra are built from four crystallographically distinct Pr atoms. As illustrated at the top of Figure 4, the tetrahedra share Pr1−Pr2 edges as well as, alternately, Pr3−Pr3 and Pr4−Pr4 edges and are centered by two unique interstitial atom positions. The chains all lie in layers when viewed along $\bar{b}$, but these actually run in alternate directions when viewed along [001], Figure 5. At $z = 0$ they extend along the [1$\bar{1}$0] direction, and at $z = 0.5$ they run along [110], the sets being related by 2-fold rotation and screw axes at $z = {}^1/_4$ that lie parallel to b. As shown in the bottom of Figure 4, the Pr chains are surrounded by seven crystallographically unique Br atoms that bridge the four open edges of the tetrahedra and occupy exo sites on all Pr atoms. Br1 and Br3 each simultaneously bridge two edges (Pr1−Pr3, Pr1−Pr4 and Pr2−Pr3, Pr2−Pr4, respectively) in the same chain, similar to Br3 and Br4 in $Na_2Pr_4Br_9NO$. The Br4 and Br5 atoms bridge Pr1−Pr3 and Pr2−Pr4 edges and also bond exo (i−a) to Pr2 and Pr1 vertices, respectively, in the neighboring parallel chain in the same plane (compare Br1 and Br6 in $Na_2Pr_4Br_9NO$). In a contrary manner, two i−a bromines bond between chains with different orientations and z: Br2 and Br6 atoms over the Pr1−Pr4 and Pr2−Pr3 edges of tetrahedra and outer to Pr3 and Pr4 in the other layer, respectively. Finally, Br7 bridges Pr1−Pr3 edges (i−i) in two chains of tetrahedra with different orientation (Figure 6). The structure incorporates only one additional halogen per formula unit relative to Gd_2Cl_3N (= $Gd_8Cl_{12}N_4$), which has linear (not folded) chains of tetrahedra so that the halogen cannot bridge edges of adjoining tetrahedra (as do Br1 and Br3, above).

The coordination polyhedra about Pr1, Pr2, and Pr4 are monocapped trigonal prisms, each with two N/O (2.30−2.36 Å) and five Br atoms (2.89−3.37 Å) as direct neighbors. Pr3 centers a bicapped trigonal prisms and is surrounded by two N/O (2.30, 2.41 Å) and six Br atoms (3.03−3.33 Å). Each Pr has at least one bond to Br that is longer than normal (≥3.19 Å vs 2.95 Å from crystal radii[16]). A short Br1···Br2 distance of 3.408(2) Å between chains is noteworthy. The average Pr−Z distance, 2.34 Å in both of these phases, compares reasonably well with ~2.27 Å in Gd_2Cl_3N and ~2.37 Å in Sm_4OCl_6 when appropriate size differences for the cations are included. It was not possible to discern whether there is any order in the N and O occupancies of the tetrahedra.

Both $Na_2Pr_4Br_9NO$ and $Pr_8Br_{13}N_3O$ are structurally and electronically similar to each other and also related to α-Gd_7Cl_3N and α-Y_2Cl_3N. All of these contain edge-sharing M_4Z tetrahedra in infinite chains, but they are arranged in three different ways. The shared edges have the smaller M−M distances: 3.54 Å in $Pr_8Br_{13}N_3O$ and 3.56 Å in $Na_2Pr_4Br_9NO$, and these are, interestingly, less than the 3.63 Å average in $Na_2Pr_4Cl_9O_2$, even disregarding the presence of one extra electron that may remain in the latter. Our observed Pr−Pr distances are even shorter than those in Pr metal (3.64 Å), and correspond to Pauling bond

(19) Atom positions in the present $Na_2Pr_4Br_9NO$ are reported with a different origin and halogen numbering, which may be converted to those in ref 5 by ${}^1/_2 - x, y, -z$ (and unit translations) and halogen renumbering 4, 5, 2, 1, 3, 6, respectively.

(20) Meyer, G. Private communication, 1995.

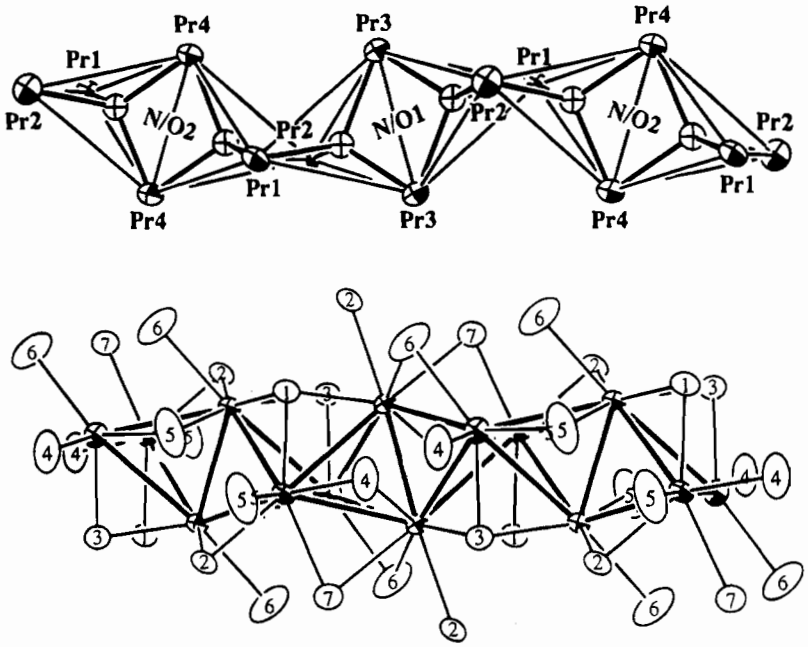

Figure 4. Top: The $^{1}_{\infty}[Pr_{4/2}(O/N)]$ chain in $Pr_8Br_{13}N_3O$. Bottom: The same chain with bromine atoms added (98%).

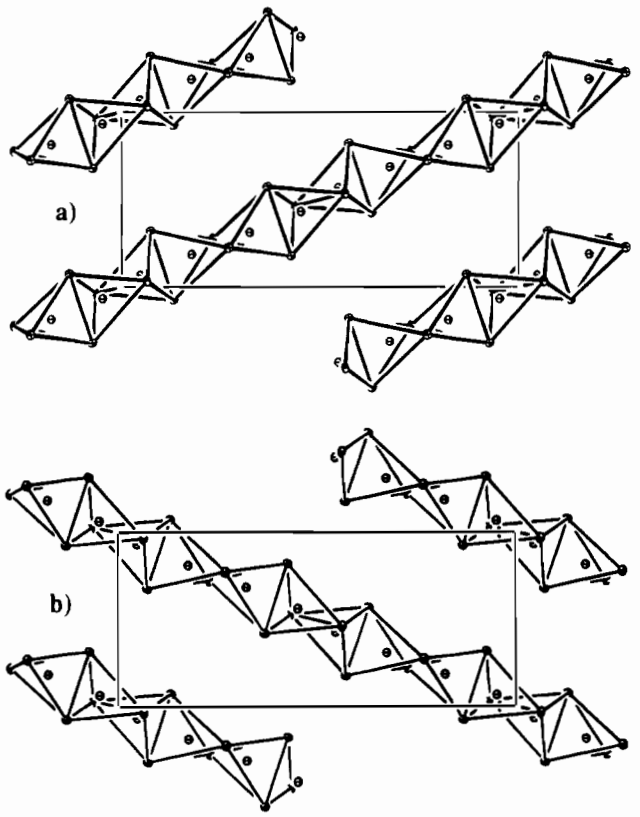

Figure 5. [001] views of the layers of chains in $Pr_8Br_{13}N_3O$ at (a) $z = 0$ and (b) $z = 0.5$. $\bar{a}$ is horizontal (90%).

orders of ca. 0.37. However, there are numerous examples of this behavior in compounds of normal-valent metals—matrix effects of a sort—in which anions are shared between cations but metal–metal bonding is unlikely as no electrons are available for this purpose. Similar to the colorless α-Gd_2Cl_3N, $Na_2Pr_4Br_9NO$ crystals are green and transparent while the dark crystals of $Pr_8Br_{13}N_3O$ powder to a nearly white material. This behavior and the characteristics of the syntheses suggest that these are closed shell compounds, "simple" salts that contain normal-valent cations and bromide, nitride and oxide anions. It is particularly noteworthy that they both require mixed interstitials to achieve stability and normal valence states, a feature that has evidently not been seen before in "cluster" compounds. The proportions must be closely correlated with the bromide content, and this, with the needs of a favorable structure and all of the edge-bridging and exo bonding requirements of the Pr_4Z units. The zigzag character of the chains derives from, or follows, the inter-tetrahedra bonding of bromine along the chains on adjoining edges and faces (i.e., Br3, Br4 in Figure 1; Br1, Br3 in Figure 4). The contrast with the simplicity of Gd_2Cl_3N is notable, which may be represented as $Gd_{4/2}N(Cl^{i-a})_2Cl^{i-i}$.

Notwithstanding, an alternate description of these structures is also possible starting with metal-rich cluster compounds. These chains of tetrahedra can also be derived from trans-edge-sharing Pr_6 octahedra that have been elongated in the chain direction to the extent that a trans-bond normal to the shared edges forms between the former apices, and two interstitial cavities are thereby defined rather than one. (See the illustration in the Table of Contents.) The shortest shared edges are again internally bridged only by N or O. This mode yields $Pr_2Pr_{4/2}Br_8Br_2Z_2 = Pr_4Br_{10}Z_2$ if all open edges are bridged by separate bromide and Br^{i-a} functions apply between chains, or $Pr_4I_6Z_2$ if the first group of bromine atoms bridge edges of adjoining tetrahedra. The corresponding empirical formulae for the new compounds are similar, $Na_2Pr_4Br_9Z_2$ and $Pr_4Br_{6.5}Z_2$, or $Pr_4Br_7Z_2$ for the first without NaBr. The differences in bromide proportions reflect more subtle changes in functionality and interchain bridging.

Conversely, the structures described here may be directly related to condensed octahedral cluster phases like Pr_4I_5Ru. If the chains in Figure 1 are made linear and compressed, the pairs of Br1, Br6 atoms will merge into single atoms that bridging edges of two adjoining clusters, the trans Pr3-Pr3 bond will break, and a single interstitial cavity will form in Pr_4Br_4Z. Interbridging these by X^{i-i} atoms normal to the view, together with connection of parallel chains in the page via Br^{i-a} bonds that are already present (Figure 1), gives the connectivity of the known Pr_4I_5Ru![10] Furthermore, if the two adjacent N/O atoms that bridge the shared Pr1-Pr2 edges are also regarded as ligands, we then have an edge-bridged M_6X_{12} $(Pr_6Br_{10}(N,O)_2)$

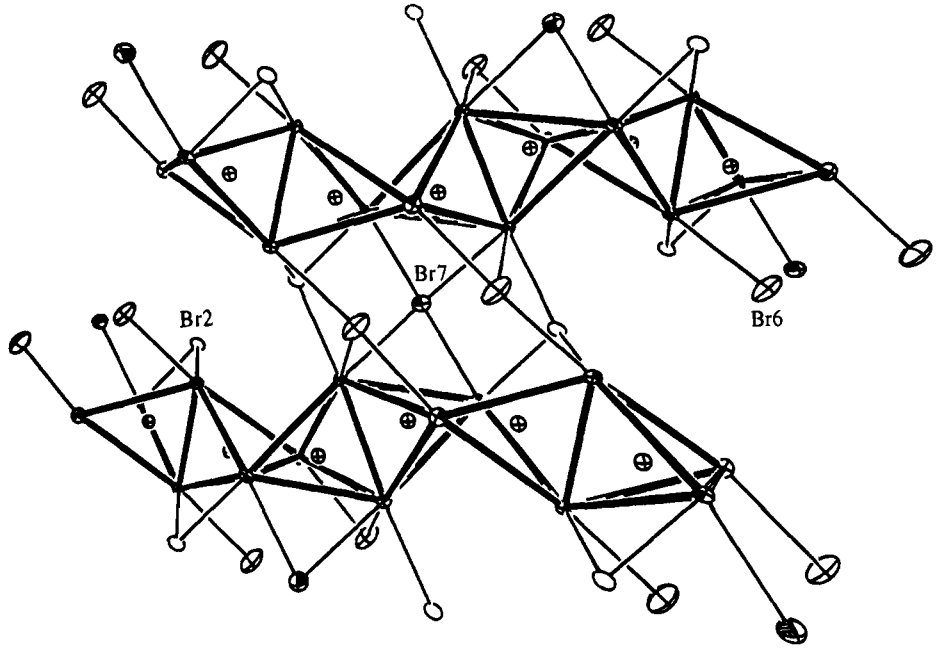

Figure 6. $Br7^{i-i}$ atoms (shaded) bridging between crossed chains in layers of $Pr_8Br_{13}N_3O$ at different z (vertical). Br2 and Br6 (crossed) are also i−i in one chain and exo to a Pr vertex in a second, nonparallel chain.

cluster, the basic unit of most cluster compounds. These ligands are all shaded gray in the figure in the Table of Contents. Such a direct process nicely illustrates more of the borderline between metal−metal-bonded systems and "simple" salts.

Acknowledgment. This work was supported by the National Science Foundation, Solid State Chemistry, via Grant DMR-9207361, and was carried out in the facilities of the Ames Laboratory. M.L. thanks the Alexander von Humboldt Foundation (Bonn, Germany) for the support of a Feodor Lynen Fellowship.

Supplementary Material Available: Tables of data collection and refinement details and of anisotropic atom displacement parameters for the two structures (Tables S1−S3) and a Fourier map of the sodium environment in $Na_2Pr_4Br_9NO$ (4 pages). Ordering information is given on any current masthead page.

IC941420Q